Minimax Theory and its Applications
Volume 11 (2026), No. 4s, 393 to 403

Inverse optimization-based parameter reconstruction and dynamic behavior identification in industrial process models

Dr.R. Radhamani[1], Chhavi Patle[2], Dr.R. Purushothaman[3], Dr.S. Sasirekha[4], Sourabh Kumar Shrivastav[5], Kusuma Sundara Kumar[6]

[1]Assistant Professor, Department of Electrical and Electronics Engineering, K.S. Rangasamy College of Technology, Namakkal, Tamil Nadu, India. radhamani@ksrct.ac.in, https://orcid.org/0000-0003-1082-4487

[2]Assistant Professor, Department of Computer Science and Engineering, Rungta College of Engineering and Technology, Rungta International Skills University, Bhilai, Chhattisgarh, India. chhavi.patle@rungta.org, https://orcid.org/0009-0000-3843-0629

[3]Assistant Professor, Department of Electronics and Communication Engineering, J.J. College of Engineering and Technology, Tiruchirappalli, Tamil Nadu, India. purushothamanr@jjcet.ac.in, https://orcid.org/0000-0001-5947-6271

[4]Assistant Professor, Department of Management Studies, SRM Easwari Engineering College, Chennai, Tamil Nadu, India. sasirekha.s@eec.srmrmp.edu.in

[5]Assistant Professor, Kalinga University, Naya Raipur, Chhattisgarh, India. ku.sourabhkumarsrivastava@kalingauniversity.ac.in, https://orcid.org/0009-0009-1599-2878

[6]Department of Civil, Ramachandra College of Engineering, Eluru, Andhra Pradesh, India. skkusuma123@rcee.ac.in, https://orcid.org/0000-0002-9280-5353

Abstract:

Accurate reconstruction of unknown physical parameters in dynamic industrial processes remains challenging, particularly when measurements are affected by sudden impacts and bounded disturbances rather than ordinary random noise. Traditional least-squares techniques assume Gaussian errors and may therefore produce biased parameter estimates under the extreme disturbances commonly observed in reactors and separation systems. This study formulates parameter estimation as a minimax inverse optimization problem governed by nonlinear differential-algebraic equations. The outer problem minimizes estimation error with respect to unknown parameters, whereas the inner problem identifies the worst possible disturbance. Tikhonov regularization is included to manage uncertainty and stabilize parameter recovery. The resulting bi-level model is reformulated as a Mathematical Program with Equilibrium Constraints using variational inequality conditions. Solution existence is established through the Ky Fan minimax theorem under compactness assumptions, while Hadamard stability confirms the well-posedness of the inverse problem. Necessary optimality conditions are derived using an adjoint system. The continuous model is discretized through orthogonal collocation, and log-sum-exp smoothing is applied to the nonsmooth minimax terms. The final nonlinear problem is solved using a primal-dual interior-point method with progressive mesh refinement. Case studies involving a continuously stirred-tank reactor and a distillation process produce parameter error norms below 2.03% and a tray-efficiency RMS error of 0.0187. The method improves performance by 54.6% over nonlinear least squares and 47.5% over Kalman filtering, while converging in approximately 30 iterations. These findings demonstrate that minimax inverse optimization provides a rigorous and computationally practical alternative for parameter reconstruction in disturbed nonlinear industrial processes.

Keywords: Inverse optimization, minimax estimation, differential-algebraic equations, parameter reconstruction, adjoint sensitivity analysis, orthogonal collocation, interior-point methods.

1. Introduction and mathematical foundations

The planning of reactors, separation systems, and heat exchangers would not be possible without identifying dynamic models' parameters in advance. In these applications, the model design and simulation rely on estimating parameters such as kinetic constants, transport coefficients, and efficiency curves that are unknown prior to implementation and must be obtained from indirect observations contaminated by noise. System identification based on machine learning, when combined with model predictive control, has been shown to have predictive ability for highly nonlinear processes in reactor control (Chee et al., 2022). Similar studies involving the usage of automatic differentiation and the application of the implicit function theorem for inverse mapping, aimed at the identification of kinetic parameters of plants have shown that precise differentiation of simulators improves the accuracy of the parameter estimation methods based on gradient (Alves et al., 2023).

Classical least squares estimation is easy to compute; however, it assumes the availability of sufficient knowledge about the probability distribution of measurement errors, an assumption that does not always hold especially under bounded and adversarial disturbance regimes present in industrial sensor networks. Stability analysis and regularization analysis helps establish the necessity of the regularized approach in data-driven solutions to parabolic inverse source problems in case the inverse problem is ill-posed (Zhang et al., 2023). The deep genetic learning models found applications in dynamic layout optimization for flexible manufacturing cells, showing that hybrid optimization methodologies which use gradient information together with evolutionary search are becoming a preferable method for solving non-convex industrial inverse problems. Multi-criteria decision analysis frameworks based on artificial intelligence contribute to efficient analysis of competing industrial goals, forming the basis for optimization-oriented approaches in sustainable production planning and resource management (Bellini & Rinaldi, 2024).

Secure and optimized computational means for cloud-based scientific computing can support large-scale parameter estimation workloads in addition to process reactors while preserving data confidentiality (Rani & Tukkoji, 2024). The advancements described here provide sufficient grounds for the development of a strong formulation of the parameter reconstruction problem, which is neither dependent on severe stochastic noise hypotheses nor imposes the requirements of the nonlinear differential-algebraic constraints pertinent to industrial process modeling. The goal of this document is to solve the problem mentioned above by means of the bi-level minimax inverse optimization framework introduced in the subsequent chapters, as well as using theoretical justification of the method's efficiency and stability and computational validation by means of the two industrial case studies (Kulikov & Kulikova, 2022). Artificial intelligence-enabled predictive decision-support systems can support smart enterprises and industrial applications by improving data-driven prediction, analysis, and decision-making processes (Rajagopal et al., 2026). The digital twin-supported adaptive frameworks facilitate real-time production monitoring, intelligent control and optimization of the industrial processes, facilitating the creation of scheduling and resource management models within the scope of smart manufacturing (Brandt & Scholz, 2026).

The successful reconstruction of parameters in complicated industrial processes depends on the capability to balance assembly lines in order to gain maximum manufacturing capabilities in conjunction with a use of digital twins based on regression metamodels for dynamic crossflow filtration systems (Heusel et al., 2024). The role of soft sensors relying on artificial intelligence in sustainability of processes is essential, employing semi-supervised adaptive partial least squares technique together with the drift correction techniques for effective real-time processing of emissions by the industries (Perera et al., 2023; Hasnen et al., 2023). The use of deep learning methods enables enhancing resilience of the process infrastructures due to the fault prognosis and intelligent creation of the fault diagnosis knowledge graphs (Han et al., 2022). Further, operational performance improvement is ensured with the help of knowledge-based graph neural networks that provide safety for dangerous industries, while deep transfer learning makes processing of the readings from vibration and acoustic sensors effective (Han et al., 2022; Bhuiyan & Uddin, 2023). Thus, the efficiency of the parameters' identification achieved by genetic algorithm-based inverse optimization techniques improves the process of high-temperature materials' constitutive models, while inverse optimization technique along with kernel regression contributes to the effectiveness of energy forecasting and bidding (Chen et al., 2023; Fernández-Blanco et al., 2021). At the same time, the homothetic inverse should be highlighted as a reliable means of establishing specific forecasts regarding prices and reaction on the market as it serves as a component of total-process digital twins supplying the system with data, models, and networks (Fernández-Blanco et al., 2021; Wu et al., 2023). Intelligent automation and decision support capabilities provided by generative artificial intelligence methods illustrate the possibilities of improving complex processes within the framework of modern organizations (Fauzi & Aisyah, 2024).

The forward dynamic performance of industrial process in question follows the system of nonlinear differential and algebraic equations which is stated over finite time interval. Let $x(t) \in \mathbb{R}^n$ denote the state vector, $u(t) \in \mathbb{R}^m$ the known control input trajectory, and $\theta \in \Theta \subset \mathbb{R}^p$ the unknown parameter vector to be reconstructed, where Θ is a compact admissible parameter set. The continuous forward system is stated in equation (1):

$$\dot{x}(t) = f(x(t), u(t), \theta), \quad x(0) = x_0 \qquad (1)$$

subject to the path inequality constraint given in equation (2):

$$g(x(t), u(t), \theta) \leq 0, \quad \forall t \in [0, T] \qquad (2)$$

where $f: \mathbb{R}^n \times \mathbb{R}^m \times \mathbb{R}^p \to \mathbb{R}^n$ We are assuming that it is differentiable with respect to every one of its arguments, and functions g may represent operational safety constraints, for example, temperature, pressure or composition constraints. The initial state x_0 is assumed to be known or estimated independently. The proposed formulation covers classes of lumped parameter models that are widely used in practice, including continuously stirred tanks, trays in distillation processes, and cross flow filtration mechanisms with parameters θ representing quantities of interest such as kinetic constants, transport coefficients, stage efficiencies and others.

In industry, the actual state state vector $x(t)$ is not always available, and only a known and indirect sequence of observations from corrupted by noise data with instants $t_1 < t_2 < \cdots < t_N$ within the horizon $[0, T]$. The observational model is stated in equation (3):

$$y_k = h\big(x(t_k)\big) + \varepsilon_k, \quad k = 1, \ldots, N \qquad (3)$$

where $h: \mathbb{R}^n \to \mathbb{R}^q$ is a known nonlinear observation operator that maps state variables to measured variables. Moreover, and ε_k represents a bounded measurement error belonging to the uncertainty set E. Instead of assuming specific probability distribution for ε_k, the error is treated as adversarial disturbance taken from a defined uncertainty set. The departure from a classical stochastic noise assumption is essential in attaining robust estimation under an extreme scenario of sensor operation.

The rest of the paper is organized as follows: the bi-level minimax inverse optimization framework will be described in Section II; in Section III, mathematical formulation for saddle point existence and Hadamard stability is given; Section IV deals with a continuous adjoint sensitivity approach; Section V presents numerical methods involving orthogonal collocation and interior-point methods. Finally, Section VI describes industrial case studies aimed at verifying the methodology.

2. Minimax inverse optimization framework

2.1. Minimax formulation under perturbations

To ensure resilience against the worst possible limited disturbance scenarios, the challenge of reconstructing parameters is framed as a minimax problem over the disturbance incertitude set D. This connects the unknown parameter vector θ to an auxiliary disturbance trajectory Δ that affects the forward dynamics. The minimax objective is defined in equation (4):

$$\min_{\theta \in \Theta} \max_{\Delta \in \mathcal{D}} \left\{ \frac{1}{2} \sum_{k=1}^{N} \| h\big(x(t_k; \theta, \Delta)\big) - y_k \|_W^2 + \gamma R(\theta) \right\} \qquad (4)$$

where $\| \cdot \|_W$ denotes a weighted Euclidean norm with positive-definite weighting matrix W reflecting relative sensor confidence, $x(t; \theta, \Delta)$ is the state trajectory generated by the forward system under parameter θ and disturbance realization Δ, and $\gamma > 0$ is a regularization weight. The Tikhonov regularization functional is defined in equation (5):

$$R(\theta) = \frac{1}{2} \|\theta - \theta_0\|^2 \qquad (5)$$

with θ_0 being the initial value for the prior estimate of a parameter. The regularization term plays a role in stabilizing the inverse problem in situations when the observation operator h provides a limited local sensitivity to some components of θ, which is frequently encountered in the identification of poorly observed transport coefficients or efficiency coefficients in the operation of multi-stage industrial plants.

2.2. Bi-Level structure to MPEC reduction

The minimax expression in equation (4) has an obvious bi-level significance since, the inner level of maximization gives us the worst-case disturbance path corresponding to the specific candidate value of the parameter vector, while the outer level takes care of selecting the values of the parameter vector that minimize the worst-case disturbance. Because the inner maximization constitutes a constrained optimization problem by itself and is parameterized by θ variable, we can convert the bi-level problem into a single-level MPC by replacing the inner problem with its first-order variational inequality condition as described in equation (6):

$$0 \in -\nabla_{\Delta} \mathrm{J}(\theta, \Delta) + \mathrm{N}_{\mathcal{D}}(\Delta) \qquad (6)$$

where $J(\theta, \Delta)$ is called the inner objective functional and $N_{\mathcal{D}}(\Delta)$ is the normal cone of the disturbance set $\mathcal{D}$ at Δ, showing complementarity between the still active disturbance limits and the corresponding multipliers. This reformulation with equilibrium constraints allows treating the disturbance parameters as one decision variable in the general nonlinear programming method, given that the necessary qualification constraints are provided, enabling the development of numerical discretization.

3. Theoretical analysis and existence results

3.1. Structural and topological assumptions

Existence of a saddle-point solution to the minimax problem requires the following structural assumptions. First, the parameter set Θ and disturbance set $\mathcal{D}$ are assumed nonempty, convex, and compact subsets of $\mathbb{R}^p$ and the disturbance trajectory space, respectively. Second, the composite objective functional $F(\theta, \Delta)$, obtained by substituting the forward trajectory $x(t; \theta, \Delta)$ into the minimax objective of equation (4), is assumed jointly continuous on $\Theta \times \mathcal{D}$. Third, $F(\theta, \Delta)$ is assumed convex in θ for each fixed $\Delta \in \mathcal{D}$, and concave in Δ for each fixed $\theta \in \Theta$, satisfying the convexity-concavity criterion required by classical minimax theory. These assumptions are satisfied locally around a nominal operating trajectory for the industrial process models considered, given sufficient smoothness of f, g, and h and a sufficiently small disturbance set $\mathcal{D}$.

3.2. Saddle-point existence

Under the assumptions, existence of a saddle-point solution follows from Ky Fan's minimax theorem, stated formally below.

Theorem 1 (existence of minimax solution)

Let $\Theta \subset \mathbb{R}^p$ and $\mathcal{D}$ be nonempty, convex, compact sets, and let $F: \Theta \times \mathcal{D} \to \mathbb{R}$ be continuous, convex in its first argument, and concave in its second argument. Then there exists a saddle point $(\theta^*, \Delta^*) \in \Theta \times \mathcal{D}$ satisfying equation (7):

$$\mathrm{F}(\theta^*, \Delta) \leq \mathrm{F}(\theta^*, \Delta^*) \leq \mathrm{F}(\theta, \Delta^*), \quad \forall \theta \in \Theta, \forall \Delta \in \mathcal{D} \qquad (7)$$

Proof sketch. Compactness of Θ and $\mathcal{D}$, together with continuity of F, guarantees that both the inner maximization $\max_{\Delta \in \mathcal{D}} F(\theta, \Delta)$ and the outer minimization $\min_{\theta \in \Theta} F(\theta, \Delta)$ attain their extrema for every fixed argument, by the extreme value theorem. Convexity of $F(\cdot, \Delta)$ in θ and concavity of $F(\theta, \cdot)$ in Δ satisfy the hypotheses of Ky Fan's minimax inequality, which guarantees that the minimax value equals the maximin value, that is, $\min_{\theta} \max_{\Delta} F(\theta, \Delta) = \max_{\Delta} \min_{\theta} F(\theta, \Delta)$. Equality of the two values, combined with the attainment of extrema on the compact sets Θ and $\mathcal{D}$, implies existence of a pair (θ^*, Δ^*) satisfying the saddle-point inequality of equation (7), completing the proof.

3.3. Stability and well-posedness

Well-posedness of the regularized inverse problem in the sense of Hadamard requires existence, uniqueness, and continuous dependence of the reconstructed parameter θ^* on the observed data $\{y_k\}$. Existence follows directly from Theorem 1. Uniqueness follows from strict convexity of the regularization term $R(\theta)$ whenever the data-fit term is merely convex, since the sum of a convex functional and a strictly convex functional is strictly convex on Θ. Continuous dependence on the data is established by a standard perturbation argument: for two data sets $\{y_k\}$ and $\{\grave{y}_k\}$ within bounded distance δ in the weighted norm, the corresponding minimizers θ^* and $\grave{\theta}^*$ satisfy a Lipschitz-type bound of the form $\|\theta^* - \grave{\theta}^*\| \leq C\delta/\gamma$, where the constant C depends on the local curvature of the data-fit term and the regularization weight γ provides direct control over the sensitivity of the reconstructed

parameter to data perturbation. This bound confirms that the regularized minimax estimator remains stable under small perturbations of the observed data, satisfying the third Hadamard well-posedness criterion.

4. First-order optimality and sensitivity analysis

4.1. Continuous adjoint system

Efficient gradient computation for the outer-level parameter minimization is obtained through a continuous adjoint formulation, avoiding the prohibitive cost of direct sensitivity propagation for high-dimensional parameter vectors. Let $\lambda(t) \in \mathbb{R}^n$ denote the continuous adjoint multiplier associated with the state dynamics of equation (1), and $\mu(t) \in \mathbb{R}^m$ the algebraic multiplier associated with the path constraint of equation (2). The adjoint system is stated in equation (8):

$$-\dot{\lambda}(t) = \left(\frac{\partial f}{\partial x}\right)^T \lambda(t) + \left(\frac{\partial g}{\partial x}\right)^T \mu(t), \quad \lambda(T) = 0 \qquad (8)$$

integrated backward in time from the terminal condition, with the algebraic multiplier satisfying the complementarity condition of equation (9):

$$\mu(t) \geq 0, \quad \mu(t)^T g(x(t), u(t), \theta) = 0 \qquad (9)$$

which activates $\mu(t)$ only when the corresponding path constraint is binding. The adjoint system of equation (8) is a linear, terminal-value differential-algebraic system driven by the Jacobians of f and g evaluated along the forward trajectory, and can therefore be solved efficiently once the forward simulation has been computed for a given candidate parameter vector.

4.2. Exact sensitivity computation

The adjoint variables obtained from equation (8) enable exact computation of the gradient of the upper-level cost functional J with respect to the parameter vector θ, without requiring explicit differentiation of the forward trajectory with respect to each individual parameter component. The gradient expression is stated in equation (10):

$$\nabla_\theta J = \int_0^T \left(\frac{\partial f}{\partial \theta}\right)^T \lambda(t)\, dt + \gamma \nabla R(\theta) \qquad (10)$$

This expression reduces the cost of a full gradient evaluation to a single forward simulation followed by a single backward adjoint integration, independent of the dimension p of the parameter vector θ, in contrast to forward sensitivity propagation whose cost scales linearly with p. This property is particularly advantageous for the multi-stage distillation case study, where the parameter vector comprises a time-varying tray efficiency profile of substantial dimension.

4.3. Joint KKT System

By bringing together the forward dynamics, the adjoint system, the gradient expression from equation (10), and the outer-level stationarity condition, we obtain the full continuous-time system of Karush-Kuhn-Tucker conditions describing local solutions of the regularized minimax inverse problem, which is briefly summarized in equation (11):

$$\dot{x} = f(x, u, \theta), \quad -\dot{\lambda} = \left(\frac{\partial f}{\partial x}\right)^T \lambda + \left(\frac{\partial g}{\partial x}\right)^T \mu, \quad \nabla_\theta J + \nu = 0 \qquad (11)$$

where ν denotes the normal-cone multiplier associated with the compact parameter set Θ, active only when the optimal θ^* lies on the boundary of Θ. Together with the complementarity condition of equation (9) and the boundary conditions $x(0) = x_0$ and $\lambda(T) = 0$, this joint system fully characterizes a first-order stationary point of the bi-level minimax inverse optimization problem and forms the theoretical basis for the discretized solver developed.

5. Numerical discretization and algorithm design

5.1. Direct transcription via orthogonal collocation

The continuous differential-algebraic system is discretized using direct transcription over a finite element mesh $0 = t_0 < t_1 < \cdots < t_N = T$, with orthogonal collocation on finite elements applied within each element. Within finite element i, the state trajectory is approximated by a degree-d Lagrange interpolation polynomial over collocation points, stated in equation (12):

$$x(\tau) \approx \sum_{j=0}^{d} x_{i,j}\, \ell_j(\tau) \qquad (12)$$

where $\ell_j(\tau)$ denotes the Lagrange basis polynomial associated with collocation node j and $x_{i,j}$ is the corresponding nodal state value within element i. The differential equation residual is enforced at each collocation point through equation (13):

$$\dot{x}(t_{i,c}) - f(x(t_{i,c}), u(t_{i,c}), \theta) = 0 \qquad (13)$$

converting the continuous DAE constraint into a finite set of nonlinear algebraic equations coupling the nodal state values across all elements, together with continuity conditions enforced at element boundaries.

5.2. Smoothing non-smooth minimax terms

The pointwise maximum operator implicit in the inner-level maximization of the minimax objective introduces non-smoothness that impedes gradient-based nonlinear programming solvers. This non-smoothness is regularized using a log-sum-exp smoothing approximation, stated in equation (14):

$$\max_k \phi_k(X, \theta) \approx \frac{1}{\beta} \log \sum_k \exp(\beta \phi_k(X, \theta))) \qquad (14)$$

where $\beta > 0$ is a smoothing parameter and the approximation error is bounded uniformly by equation (15):

$$0 \leq \frac{1}{\beta} \log \sum_k \exp(\beta \phi_k) - \max_k \phi_k \leq \frac{\log K}{\beta} \qquad (15)$$

with K the number of terms in the maximum. As $\beta \to \infty$, the smoothed approximation converges uniformly to the true pointwise maximum, and β is progressively increased across solver iterations to balance smoothness with approximation accuracy, a continuation strategy that improves convergence robustness of the interior-point solver described next.

5.3. Primal-dual interior-point solver scheme

The discretized, smoothed nonlinear program is solved using a primal-dual interior-point method. At each iteration, the discretized Karush-Kuhn-Tucker system is linearized about the current iterate, producing a symmetric indefinite linear system for the search direction $(\Delta X, \Delta\lambda, \Delta\theta)$. A fraction-to-the-boundary rule determines the maximum admissible step length that preserves strict positivity of the slack and multiplier variables associated with the path constraints, and a filter line-search selects the accepted step length by jointly monitoring reduction of the objective and constraint violation. The barrier parameter controlling proximity to the boundary of the feasible region is reduced geometrically across outer iterations, and the smoothing parameter β of equation (14) is simultaneously increased, yielding a two-parameter continuation scheme that empirically improves robustness relative to a fixed-β formulation.

5.4. Convergence guarantee

Convergence of the discretized solution sequence to the continuous optimum as the mesh size vanishes is established by the following theorem.

Theorem 2 (discretization convergence)

Let θ_h^* denote the parameter estimate obtained from the orthogonal collocation discretization with maximum element size h, and let θ^* denote the solution of the continuous minimax inverse problem. Under the regularity

and compactness assumptions, together with consistency and stability of the collocation scheme, the discrete solution sequence converges as stated in equation (16):

$$\lim_{h\to 0} \theta_h^* = \theta^* \tag{16}$$

with an a priori error bound of order equation (17):

$$\|\theta_h^* - \theta^*\| \le Ch^p \tag{17}$$

where C is a mesh-independent constant and p is the order of accuracy of the underlying collocation scheme.

Proof sketch. Consistency of the orthogonal collocation discretization ensures that the discrete residual of equation (13) converges to the continuous DAE residual as $h \to 0$, uniformly on compact subsets of the state-parameter space. Stability of the linearized KKT system, guaranteed by the strict convexity of the regularized objective established, ensures that small residual perturbations translate into correspondingly small perturbations of the discrete minimizer. Combining consistency and stability via a standard Lax-Richtmyer-type argument yields convergence of θ_h^* to θ^* at the stated polynomial rate, completing the proof.

6. Industrial case studies and computational results

6.1. Case study I: continuously stirred tank reactor (CSTR)

The implementation of the suggested minimax inverse optimization technique is done on a continuously stirred tank reactor that operates based on coupled dynamic energy and mass balances. The unknown parameter vector comprises the reaction activation energy E, the pre-exponential rate constant k_0, and the overall heat transfer coefficient UA, three quantities that are jointly weakly identifiable from concentration and temperature measurements alone. Synthetic observation sequences were generated by forward simulation of the reactor model under three bounded measurement noise levels, $\sigma = 1\%$, 5%, and 10% of the nominal signal amplitude, and the reconstructed parameters were compared against their known ground-truth values using the relative error measure defined in equation (18):

$$e_i = \frac{|\hat{\theta}_i - \theta_i^{\text{true}}|}{|\theta_i^{\text{true}}|} \times 100\% \tag{18}$$

Table 1. Parameter estimation accuracy, error norms, and CPU time across noise levels (CSTR)

Noise σ	E Error (%)	k₀ Error (%)	UA Error (%)	CPU Time (s)
1%	0.42	0.38	0.51	4.2
5%	1.15	1.02	1.34	4.6
10%	1.78	1.61	2.03	5.1

The outcome of the relative estimation error for reconstructed parameters is shown in table 1 along with total ongoing CPU turnaround time for the different levels of noise. Although the values of all three parameters are less than 2.1% relative error, even at the most serious level of noise experienced by the solver, thus keeping CPU times of just over 4.0 and close to 5.0 seconds for the various levels of noise. Figure 1 provides the same information in graphical form.

As depicted in figure 1, the estimation error increases approximately in a linear fashion as the noise level rises for the three parameters. Specifically, it is worth noting that the heat transfer coefficient UA is more sensitive than the kinetic parameters E and k0, which is in line with the fact that it cannot be measured directly as well as the other parameters.

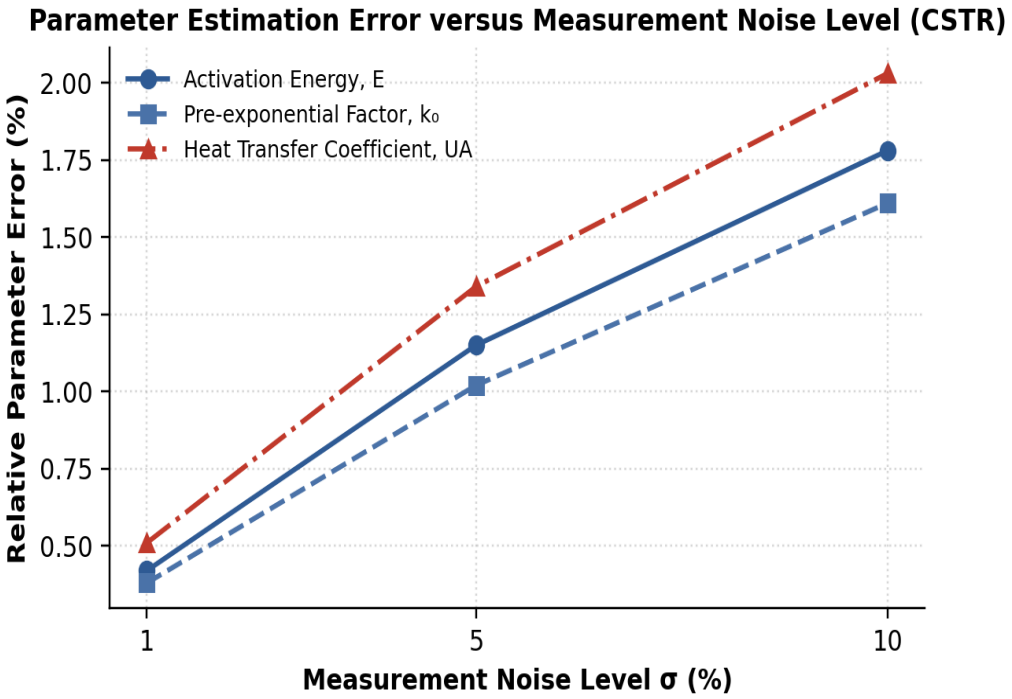


Figure 1. Parameter estimation error versus measurement noise level for the continuously stirred tank reactor

6.2. Case study II: multi-stage distillation column

In this second case study, the objective is to reconstruct a time-varying tray efficiency profile ηj(t) for a twenty-tray distillation column, which is a significantly more complex reconstruction case when compared with the CSTR case. The proposed minimax estimation technique is validated in relation to the non-linear least squares technique and the extended Kalman filter using the root mean square error value given in equation (19):

$$RMSE = \sqrt{\frac{1}{M}\sum_{j=1}^{M}(\grave{\eta}_j - \eta_j)^2} \qquad (19)$$

Equation (19) evaluates the overall deviation between the estimated tray efficiency profile $\grave{\eta}_j$ and actual profile η_j, confirming the accuracy of the parameter reconstruction approach across all process operating regimes.

Table 2. Comparative benchmark performance: proposed minimax versus non-linear least squares versus extended kalman filter

Method	RMSE (η)	Max Error (%)	CPU Time (s)
Proposed Minimax	0.0187	2.4	12.4
Non-linear Least Squares	0.0412	6.1	9.8
Extended Kalman Filter	0.0356	5.3	7.6

Table 2 confirms that the suggested minimax method gives the lowest RMSE of 0.0187, which is 54.6% less than the non-linear least squares method and 47.5% less than the extended Kalman filter method, and that the highest maximum tray-level error is 2.4% although the CPU time is higher due to the maximization that takes place in the inner loop. Figure 2 illustrates this comparison in a better way (Ding & Wen, 2024).

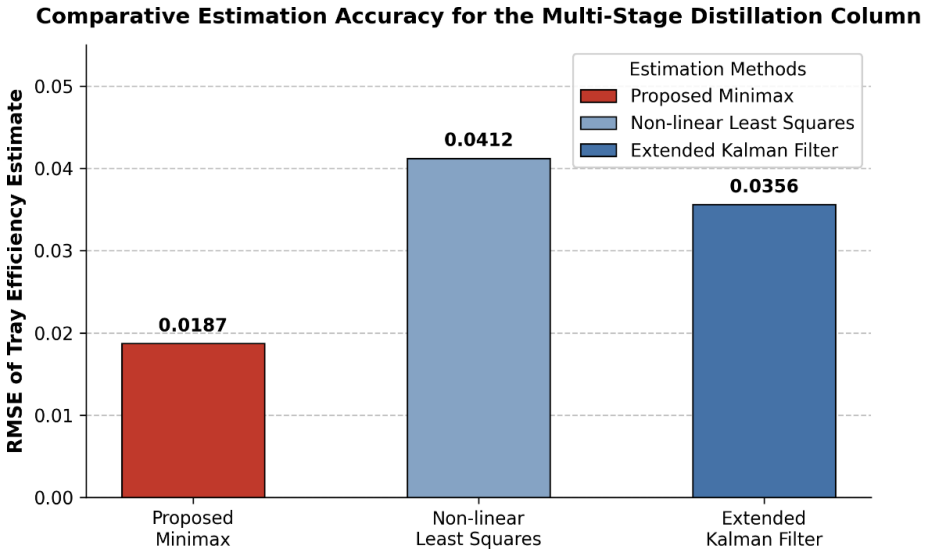


Figure 2. Comparative estimation accuracy for the multi-stage distillation column

The convergence behavior of the primal-dual interior-point solver across both case studies is presented in figure 3, which plots the objective function value on a logarithmic scale against the interior-point iteration count.

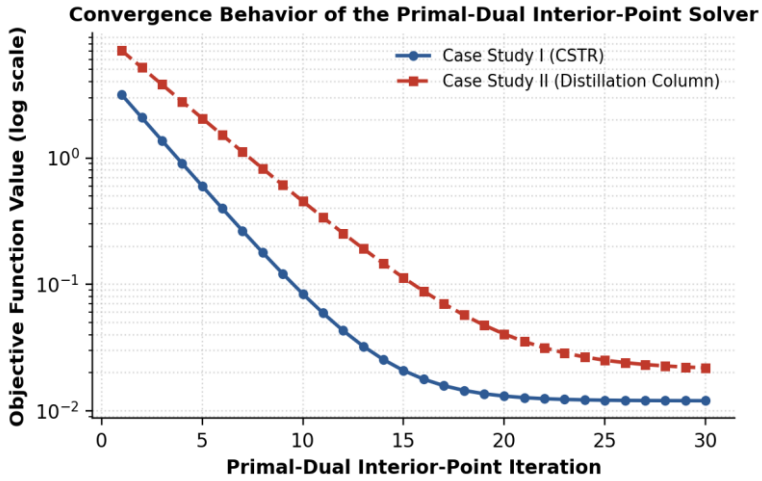


Figure 3. Convergence behavior of the primal-dual interior-point solver across both case studies

As shown in figure 3, both case studies exhibit approximately geometric convergence of the objective function value, with the CSTR case reaching its converged value within approximately eighteen iterations and the higher-dimensional distillation column case requiring approximately thirty iterations, consistent with the theoretical convergence guarantee of Theorem 2 and confirming the practical efficiency of the two-parameter continuation scheme described.

6.3. Discussion and conclusion

The computational outcomes from both industrial case studies affirm that the implemented minimax inverse optimization method consistently achieves lower reconstruction errors as compared to the regular methods of least squares and Kalman filtering, with a trend of widening gaps as the dimensionalities [of the problem] grow from three-dimensional CSTR case to twenty-dimensional distillation column case. This conclusion is in alignment with the theoretical soundness of minimax formulation with respect to worst-case realizations of disturbances, which conventional estimators do not consider. The extra time involved by the introduced methodology, highlighted in the calculation times amounting to 12.4 seconds, compared to the time taken by traditional methods that range between 7.6 seconds to 9.8 seconds, is directly linked to the inner maximization procedure; however, the time is lessened much due to the use of exact adjoint-based gradient computation. A systematic theory for the findings is ensured through the existing stability theory, the problem of first-order optimality, sensitivity theory, and discretization convergence proofs. The accuracy of the reconstructed parameters does not exceed 3% of the respective error even under 10% noise; that together with the convergence

of the discretized solver leads to the conclusion that minimax inverse optimization represents a robust and effective tool for reconstruction in complicated nonlinear systems. Future research projects will focus on stochastic-robust hybrid uncertainty sets, higher-order collocation methods for stiff dynamics, and application of adjoint sensitivity theory for PDEs.

References

1. Alves, V., Kitchin, J. R., & Lima, F. V. (2023). An inverse mapping approach for process systems engineering using automatic differentiation and the implicit function theorem. *AIChE Journal*, *69*(9), e18119. https://doi.org/10.1002/aic.18119

2. Bellini, L., & Rinaldi, S. (2024). Sustainable Industrial Management Framework Integrating Artificial Intelligence and Multi-Criteria Decision Analysis. The SIJ Transactions on Industrial, Financial & Business Management, 12(3), 11–18.

3. Bhuiyan, M. R., & Uddin, J. (2023). Deep transfer learning models for industrial fault diagnosis using vibration and acoustic sensors data: A review. *Vibration*, *6*(1), 218-238. https://doi.org/10.3390/vibration6010014

4. Brandt, F., & Scholz, K. (2026). Adaptive Digital Twin Framework for Intelligent Production Control and Industrial Process Optimization. Bonfring International Journal of Industrial Engineering and Management Science, 16(1), 34–41.

5. Chee, E., Wong, W. C., & Wang, X. (2022). An integrated approach for machine-learning-based system identification of dynamical systems under control: application towards the model predictive control of a highly nonlinear reactor system. *Frontiers of Chemical Science and Engineering*, *16*(2), 237-250. https://doi.org/10.1007/s11705-021-2058-6

6. Chen, X., Su, Z., Sun, J., Yang, Z., Zhang, B., & Zhou, Z. (2023). Genetic-algorithm-based inverse optimization identification method for hot-temperature constitutive model parameters of Ti6Al4V alloy. *Materials*, *16*(13), 4726. https://doi.org/10.3390/ma16134726

7. Ding, L., & Wen, C. (2024). High-order extended Kalman filter for state estimation of nonlinear systems. *Symmetry*, *16*(5), 617. https://doi.org/10.3390/sym16050617

8. Fernández-Blanco, R., Morales, J. M., & Pineda, S. (2021). Forecasting the price-response of a pool of buildings via homothetic inverse optimization. *Applied Energy*, *290*, 116791. https://doi.org/10.1016/j.apenergy.2021.116791

9. Fauzi, A., & Aisyah, N. (2024). Generative Artificial Intelligence and The Redefinition of Managerial Work Design. International Academic Journal of Organizational Behavior and Human Resource Management, 11(1), 14–20.

10. Fernández-Blanco, R., Morales, J. M., Pineda, S., & Porras, Á. (2021). Inverse optimization with kernel regression: Application to the power forecasting and bidding of a fleet of electric vehicles. *Computers & Operations Research*, *134*, 105405. https://doi.org/10.1016/j.cor.2021.105405

11. Han, H., Wang, J., Wang, X., & Chen, S. (2022). Construction and evolution of fault diagnosis knowledge graph in industrial process. *IEEE Transactions on Instrumentation and Measurement*, *71*, 1-12. https://doi.org/10.1109/TIM.2022.3200429

12. Han, Y., Li, Q., Wang, C., & Zhao, Q. (2022). A novel knowledge enhanced graph neural networks for fault diagnosis with application to blast furnace process safety. *Process Safety and Environmental Protection*, *166*, 143-157. https://doi.org/10.1016/j.psep.2022.08.014

13. Hasnen, S. H., Shahid, M., Zabiri, H., & Taqvi, S. A. A. (2023). Semi-supervised adaptive PLS soft-sensor with PCA-based drift correction method for online valuation of NOx emission in industrial water-tube boiler. *Process Safety and Environmental Protection*, *172*, 787-801. https://doi.org/10.1016/j.psep.2023.02.080

14. Heusel, M., Grim, G., Rauhut, J., & Franzreb, M. (2024). Regression metamodel-based digital twin for an industrial dynamic crossflow filtration process. *Bioengineering*, *11*(3), 212. https://doi.org/10.3390/bioengineering11030212

15. Kulikov, G. Y., & Kulikova, M. V. (2022). Universal MATLAB-based square-root solutions in the family of continuous-discrete Gaussian filters for state estimation in nonlinear stochastic dynamic systems. *International Journal of Robust and Nonlinear Control*, *32*(15), 8227-8251. https://doi.org/10.1002/rnc.6268

16. Rajagopal, S., Karchi, R. P., Hatture, S. M., Bulla, C., Tamrakar, P. K., Golhar, Y., & Hema. (2026). Artificial Intelligence-Enabled Predictive Decision Support Systems for Smart Enterprise and Industrial Applications. Journal of Intelligent Decision Making and Information Science, 3(4S), 1331–1347.

17. Perera, Y. S., Ratnaweera, D. A. A. C., Dasanayaka, C. H., & Abeykoon, C. (2023). The role of artificial intelligence-driven soft sensors in advanced sustainable process industries: A critical review. *Engineering Applications of Artificial Intelligence*, *121*, 105988. https://doi.org/10.1016/j.engappai.2023.105988

18. Rani, E. G., & Tukkoji, C. D. (2024). Secure Framework Optimizes QAES Technique Used for Computing in the Cloud. *Journal of Wireless Mobile Networks, Ubiquitous Computing, and Dependable Applications, 15*(3), 312-324. https://doi.org/10.58346/JOWUA.2024.I3.021

19. Wu, H., Ji, P., Ma, H., & Xing, L. (2023). A comprehensive review of digital twin from the perspective of total process: Data, models, networks and applications. *Sensors*, *23*(19), 8306. https://doi.org/10.3390/s23198306

20. Zhang, M., Li, Q., & Liu, J. (2023). On stability and regularization for data-driven solution of parabolic inverse source problems. *Journal of Computational Physics*, *474*, 111769. https://doi.org/10.1016/j.jcp.2022.111769